19th Australasian Fluid Mechanics Conference
Melbourne, Australia
8-11 December 2014

Effect on Fluctuating Lift of the Phase Lag between Vortex Sheddings from Two Tandem Circular Cylinders

M. M. Alam[1, 2], M. Zhe[1], and Y. Zhou[1]

[1]Institute for Turbulence-Noise-Vibration Interaction and Control
Shenzhen Graduate School, Harbin Institute of Technology, Shenzhen 518055, China

[2]Key Lab of Advanced Manufacturing Technology, School of Mechanical Engineering and Automation
Shenzhen Graduate School, Harbin Institute of Technology, Shenzhen 518055, China

Abstract

Flow-induced forces on two tandem circular cylinders of identical diameter are studied numerically at Reynolds number Re = 200 using finite volume method. The spacing ratio L^* (= L/D) is varied from 2 to 9, where L is the cylinder center-to-center spacing and D is the cylinder diameter. Here we mainly focus on fluctuating lift coefficient C_{Lf} of the upstream cylinder, vortex dynamics in the gap between cylinders, and phase lag ϕ between the vortex sheddings from the two cylinders for L^* larger than the critical where the co-shedding flow prevails. ϕ is indeed nonlinear function of L^*, Strouhal number (St) and convection velocity of vortices in the gap between the cylinders. We unearth that the upstream cylinder C_{Lf} is affected by both L^* and ϕ. While a larger L^* corresponds to a diminishing C_{Lf}, ϕ makes the L^*-dependent C_{Lf} variation damped-sinusoidal. The inphase and antiphase flows respectively correspond to a local maximum and minimum C_{Lf}.

Introduction

The flow interference between the cylinders is non-linear and very complex as Reynolds number (Re, based on the cylinder diameter D and the free-stream velocity U_∞) and spacing ratio L^* (= L/D, where L is the cylinder center-to-center spacing) are changed. Zdravkovich [8] reviewed the problem of flow interference between two cylinders in tandem. Three flow regimes are identified: extended-body/overshoot regime (L^* < 1.2 - 1.8), reattachment regime (1.2 - 1.8 < L^* < 3.4 - 3.8) and coshedding regime (L^* > 3.4 - 4.0). The spacing differentiating the second and third regimes is known as the critical spacing L_c^*. Measurements of fluctuating lift coefficient C_{Lf} at $Re = 6.5\times10^4$ were done by Alam et al. [1,2]. They observed that the variation in the upstream cylinder C_{Lf} at $L^* > L_c^*$ (= 4) follows a damped sine curve at different L^*. There is a definite phase lag (ϕ) between the vortex sheddings from the two cylinders ([1,7]). Experimental data (e.g., [1,2], $Re = 6.5\times10^4$) showed that ϕ varies almost linearly with an increase in L^*. Alam et al. [2] pioneered that ϕ has a significant effect on C_{Lf} of the upstream cylinder, local maxima and minima of C_{Lf} corresponding to two cylinders' vortex sheddings occurring at inphase (i.e., $\phi = 2n\pi$, where n = 1, 2, . .) and antiphase (i.e., $\phi = (2n+1)\pi$), respectively.

The objective of this work is to find the relationship between ϕ, C_{Lf} and L^* at low Re and provide an insightful physics of the relationship from 2-dimensional simulation results obtained at Re = 200. C_{Lf}, St and ϕ are estimated and presented as functions of L^*. Furthermore, to assimilate the insight into the relationship between ϕ, C_{Lf} and L^*, we extracted velocity and pressure fields and information on vortex dynamics.

Numerical Method

The governing equations for an unsteady, viscous, laminar and incompressible fluid flow with constant properties are the continuity and momentum equations expressed in Cartesian coordinate as

$$\frac{\partial u}{\partial x}+\frac{\partial v}{\partial y}=0,$$

$$\frac{\partial u}{\partial t}+u\frac{\partial u}{\partial x}+v\frac{\partial u}{\partial y}=-\frac{\partial P}{\partial x}+\frac{1}{Re}\left(\frac{\partial^2 u}{\partial x^2}+\frac{\partial^2 u}{\partial y^2}\right),$$

$$\frac{\partial v}{\partial t}+u\frac{\partial v}{\partial x}+v\frac{\partial v}{\partial y}=-\frac{\partial P}{\partial x}+\frac{1}{Re}\left(\frac{\partial^2 v}{\partial x^2}+\frac{\partial^2 v}{\partial y^2}\right),$$

where u and v are the velocity components in the x and y directions, respectively, P is the pressure and t is the time. The computations are performed using Ansys-Fluent solver. While a standard scheme and a second order upwind scheme are used to discretize pressure and velocity, respectively, the first order implicit formulation is used for time discretization. The coupling between the pressure and velocity fields are done using the SIMPLE technique.

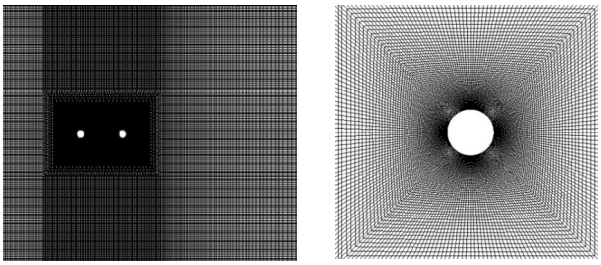

(a) (b)

Figure 1. (a) Typical grid structure in the computational domain. (b) Zoom-in view of grids around a cylinder.

The computational domain was 65D in the streamwise direction and 30D in the cross-stream direction, which gives a blockage ratio of 3.3% only. The inlet boundary was 15D away from the center of the upstream cylinder. An O-xy grid system near the cylinders and a rectangular-grid system away from the cylinders were used as shown in figure 1. The number of grids for the O-grid system was 200 in the transverse direction and 60 in the radial direction. The grid in the radial direction was denser near the cylinder surface with the nearest grid being 0.01D away from the cylinder surface. The boundary conditions are (i) $u = v = 0$ on the surfaces of the cylinders, (ii) $u = U_\infty$, and $v = 0$ at the lower and upper walls, (iii) $u = U_\infty$, and $v = 0$ at the inlet, x^* (= x/D) = -15 and (iv) $\partial u/\partial x = 0$ and $\partial v/\partial x = 0$ at the outlet, $x^* = 50$.

Grid Independence Test and Result Validation

Table 1 compares time-mean drag coefficient C_D, fluctuating (rms) drag coefficient C_{Df}, fluctuating lift coefficient C_{Lf} and St results obtained by us and others. Present data display a good accord with the data by others.

$Re = 200$	C_D	C_{Df}	C_{Lf}	St
Present	1.4	0.0346	0.48	0.195
Ding et al. [5]	1.35	0.0346	0.46	0.196
Dehkordi *et al*. [4]	1.33	--	0.53	0.195
Koda and Lien [6]	1.37	0.0345	0.49	0.190

Table 1. Comparison of C_D, C_{Df}, C_{Lf} and St for a single cylinder.

Dependence of C_{Lf} on L^* and ϕ

The simulation results obtained at $L^* = 2$ to 9 showed that while the coshedding flow appears at $L^* \geq 3.65$, the reattachment flow prevails at $L^* \leq 3.5$. So the L_c^* nestles between $L^* = 3.5$ and 3.65. A concurrent plot of ϕ and C_{Lf} of the upstream cylinder with change in L^* is presented in figure 2 for $L^* > L_c^*$. Here ϕ (open circle) is estimated from cross-correlation between fluctuating lifts of the two cylinders. ϕ at $L^* = 3.65$ is slightly higher than 2π, since L_c^* is not exactly at 3.65. For a convenient discussion, we will consider $L_c^* \approx 3.65$. C_{Lf} variation shows local maxima at $L^* = 3.65$ and 7.5 and local minimum at $L^* \approx 5.25$. The former two L^* correspond to $\phi \approx 2\pi$ and 4π, respectively, inphase shedding. On the other hand, the latter corresponds to $\phi = 3\pi$, antiphase shedding. The trend of C_{Lf} can be considered as a combination of a decreasing variation and a damped sinusoidal variation with L^*. The former variation can be assumed to be caused by L^*, while the latter is due to ϕ clearly.

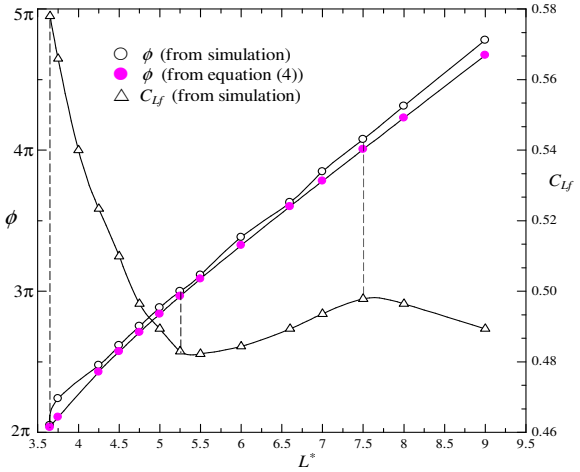

Figure 2. Relationship between ϕ, L^* and C_{Lf} of the upstream cylinder ($L^* > 3.65$).

ϕ is related to the vortex shedding from both cylinders for $L^* \geq L_c^*$ only. The convective vortices from the upstream cylinder trigger the vortex shedding from the downstream cylinder [7]. The ϕ is therefore connected to the time required for a vortex to travel from the upstream cylinder to the downstream one. Considering $\phi = 2\pi$ at $L^* = L_c^*$ regardless of Re and body shape [3], the relationship between ϕ and L^* is

$$\phi = 2\pi + \frac{2\pi\, St}{\overline{V_c}/U_\infty}(L^* - L_c^*), \quad (L^* \geq L_c^*) \tag{1}$$

where $\overline{V_c}$ is the spatial-mean velocity of the vortex between the cylinders. $\overline{V_c}$ as a function of L^* is presented in figure 3. An exponential equation fits the $\overline{V_c}$ data:

$$\overline{V}/U_\infty = 0.83 - 1.3e^{-0.35L^*}. \tag{2}$$

St is also function of L^* (not shown) and can be represented by the best fit curve equation:

$$St = 0.195 - 0.08e^{-0.35L^*}. \tag{3}$$

Now ϕ can be expressed as

$$\phi = 2\pi\{1 + \frac{0.195 - 0.08e^{-0.35L^*}}{0.83 - 1.3e^{-0.35L^*}}(L^* - L_c^*)\}, \quad (L^* \geq L_c^*) \tag{4}$$

The ϕ estimated from equation (4) and simulation agree well each other (figure 2).

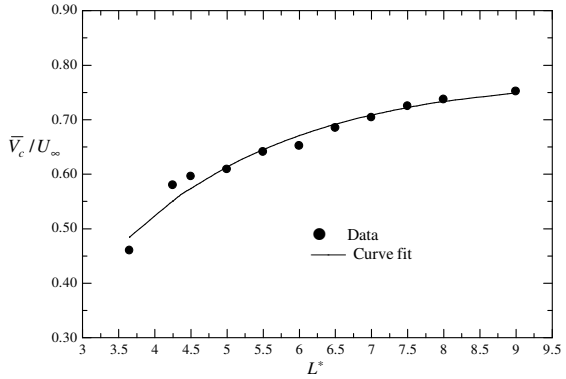

Figure 3. Variation in spatial-average convection velocity $\overline{V_c}/U_\infty$ with L^*.

Effect of L^* on the Flow Structure

Figure 4(a-e) shows contours of normalized time-mean streamwise velocity $\bar{u}^*$ ($= \bar{u}/U_\infty$, where $\bar{u}$ is the local time-mean velocity) at $L^* = 3.65$, 4.25, 5.25, 6.5, and 7.5. The region enclosed by $\bar{u}^* = 0$ is known as the recirculation region or wake bubble. With increase in L^*, (i) the wake bubble size enlarges particularly in the streamwise direction, (ii) the velocity gradient $\partial\bar{u}^*/\partial x^*$ along the wake centerline $y^* = 0$ becomes greater in the domain $\bar{u}^* > 0$. The observation implies that a larger L^* enables a greater flow from the freestream sides into the wake, which is consistent with the fact that $\overline{V_c}$ is higher at a larger L^*. Another interesting feature is that the maximum streamwise velocity $\bar{u}^*_{max}$ in the upper or lower side augments when L^* is increased. To make the observation more clear, $\bar{u}^*_{max}$ is plotted in figure 4(f).

Effect of ϕ on the Flow Structure

Since L^* mainly influences the mean flow field, the effect of ϕ on the flow field or a parameter can be understood from the instantaneous field minus mean field, for instance, $C_P - \overline{C_P}$, where C_P and $\overline{C_P}$ are the instantaneous and time-mean pressure coefficients, respectively. Figure 5(a-e) illustrates $C_P - \overline{C_P}$ field at different L^* where C_P field corresponds to the minimum C_L (solid circle) as presented in the C_L histories above each field. The solid and dashed lines in the histories represent the lift of the upstream and downstream cylinders, respectively. $C_P - \overline{C_P}$ is positive and negative on the upper and lower sides of the cylinder, respectively. It is clear that $C_P - \overline{C_P}$ magnitudes on the upper and lower sides dwindle for $L^* = 3.65$ - 5.25 where ϕ changes from inphase to antiphase and increase for $L^* = 5.25$ - 7.5 where ϕ changes from antiphase to inphase; the resultant trend follows that of C_{Lf}. A more fragrant view can be extracted from a plot of maximum and minimum $C_P - \overline{C_P}$ (i.e., $(C_P - \overline{C_P})_{max}$, $(C_P - \overline{C_P})_{min}$) as a function of L^* as presented in figure 5(f). While $(C_P - \overline{C_P})_{max}$ wanes for $L^* = 3.65$ - 5.25, $(C_P - \overline{C_P})_{min}$ augments, suggesting that flow over the upper and lower sides of the cylinder accelerates and decelerates, respectively, when ϕ changes from inphase to antiphase. The opposite phenomenon prevails at $L^* = 5.25$ - 7.5.

Contribution of L^* and ϕ to C_{Lf}

The effect of L^* and ϕ on C_{Lf} can also be extracted from a curve fitting of C_{Lf}. Based on the above results and discussion, C_{Lf} can

be written as,

$$C_{Lf} = Ae^{-\alpha L^*} + \beta \sin\left(\phi + \frac{\pi}{2}\right) + C \quad (5)$$

The coefficient A , α, β and C can be obtained from the C_{Lf} vs L^* curve. Even for a given ϕ, influence of ϕ at different L^* would be different, weaker at a larger L^*. β may therefore be again in an exponential form. C is a constant.

C_{Lf} data obtained is fitted following equation (5) as

$$C_{Lf} = 13.8e^{-1.43L^*} + 0.36\, e^{-0.2L^*} \sin\left(\phi + \frac{\pi}{2}\right) + 0.488$$

Interestingly, the last term is equal to single cylinder $C_{Lf,}$ denoted by C_{Lf0}. The equation can therefore be written as

$$C_{Lf} - C_{Lf0} = 13.8e^{-1.43L^*} + 0.36\, e^{-0.2L^*} \sin\left(\phi + \frac{\pi}{2}\right).$$

While the first term in the right hand side is associated with the effect of L^* only, the second term is connected to ϕ. Evidently the coefficient of $\sin\left(\phi + \frac{\pi}{2}\right)$ incorporates the influence of ϕ at different L^*. We will therefore call the first and second terms as the contributions of L^* and ϕ.

Original and curve fitting (equation) data are presented in figure

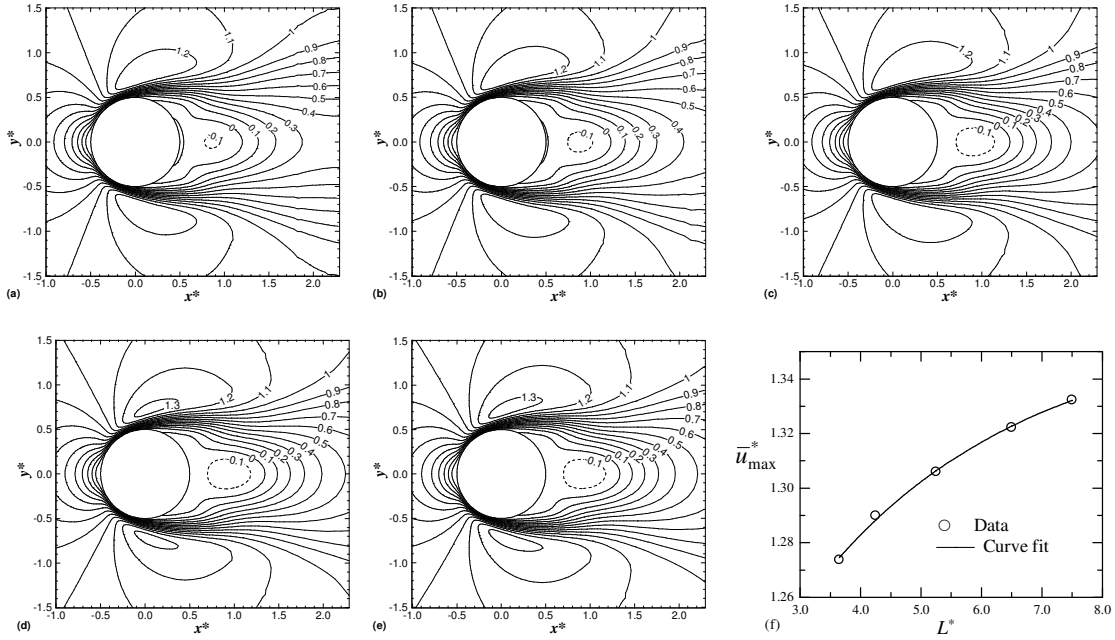

Figure 4. Contours of normalized time-mean streamwise velocity $\overline{u}^*$ at (a) L^* = 3.65, (b) 4.25, (c) 5.25, (d) 6.5, and (e) 7.5. (f) Maximum time-average streamwise velocity $\overline{u}^*_{max}$, extracted from (a - e), on the upper or lower side of the cylinder.

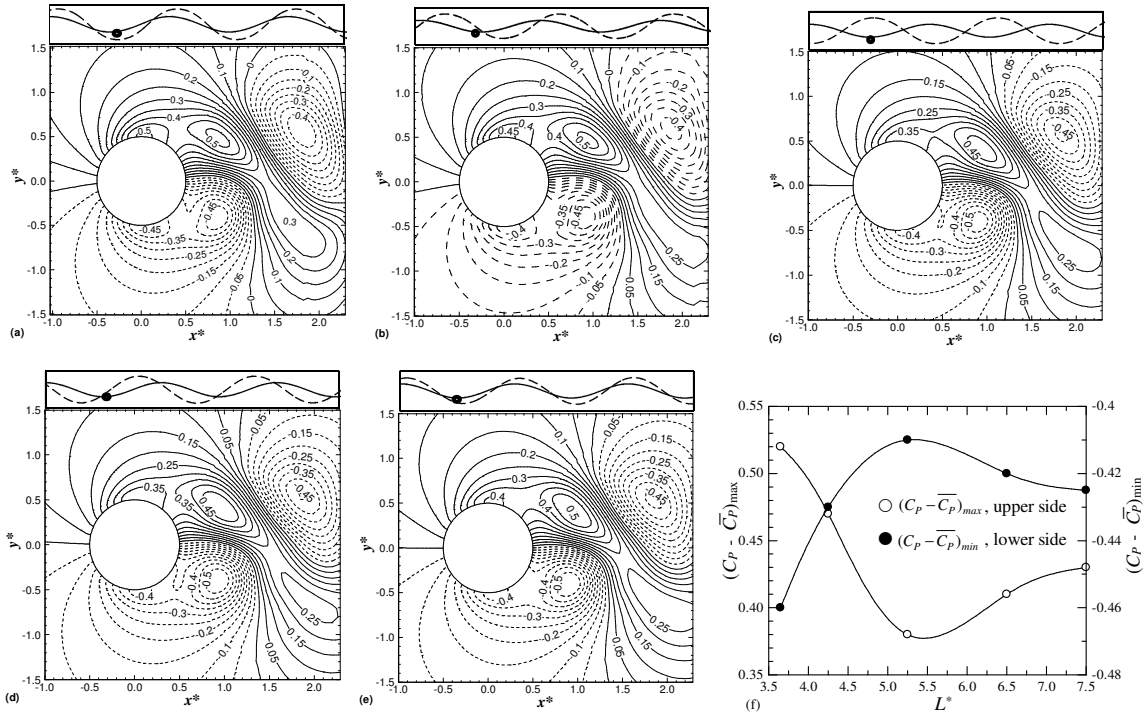

Figure 5. Contours of C_P - $\overline{C_P}$ when the upstream cylinder is subjected to the minimum lift (downward) at (a) L^* = 3.65, (b) 4.25, (c) 5.25, (d) 6.5, and (e) 7.5. (f) Variation in maximum and minimum C_P - $\overline{C_P}$ (i.e., $(C_P - \overline{C_P})_{max}$ and $(C_P - \overline{C_P})_{min}$), extracted from (a - e), on the upper and lower sides of the cylinder with increase in L^*.

6(a), showing the closeness between them. In order to get information on individual contributions of L^* and ϕ to C_{Lf}, values of first and second terms are given in figure 6(b). As seen, contribution of L^* to C_{Lf} declines rapidly, negligible at $L^* > 6$, while that of ϕ persists upto the L^* examined with the amplitude of the wave (coefficient of the sine term) diminishing slowly.

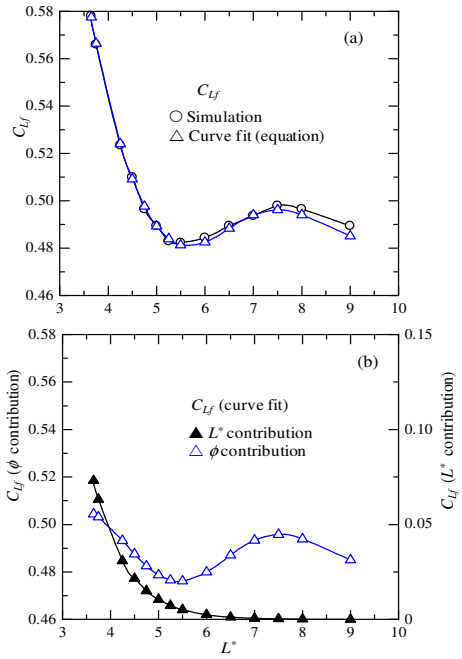

Figure 6. (a) Upstream cylinder C_{Lf} obtained from simulation and curve fit equation. (b) Contributions of L^* and ϕ to C_{Lf}.

Discussion

An increase in L^* speeds up the flow around and behind the upstream cylinder, inducing more fluid from the freestream into the gap between the cylinders. A shear layer shedding or growing is accompanied by a higher velocity and lower pressure in the shear layer. When a shear layer from the downstream cylinder grows/accelerates, it because of the low pressure pulls the fluid at the same side of the upstream cylinder and tends to accelerate the flow/shear-layer on the side. A sketch is provided in Figure 7, reflecting the overall picture of ϕ influence on the flow. For inphase sheddings of the two cylinders (figure 7a), the growing shear layer from the lower side of the downstream cylinder accelerates the same side shear layer on the upstream cylinder. In the next half cycle, the other side shear layer will accelerate. The alternating acceleration of the two shear layers of the upstream cylinder results in an enhanced C_{Lf}. When the sheddings change from inphase to antiphase, the velocity in the growing shear layer of the upstream cylinder reduces and that in other side increases, which leads to a decay in C_{Lf} with L^*. At antiphase (figure 7b), the growing shear layers of the two cylinders are in opposite sides. The growing the shear layer of the downstream cylinder therefore accelerates the flow in the non-growing shear layer of the upstream cylinder, which results in a smallest C_{Lf}. The larger the L^*, the smaller the influence of ϕ or pulling effect, as a larger L^* corresponds to a greater amount (mass) of fluid between the same-side shear layers of the cylinders.

Conclusions

Upstream cylinder C_{Lf} in the co-shedding regime is influenced by L^* and ϕ. The L^* effect causes an exponential decrease in C_{Lf}, while the ϕ effect makes the C_{Lf} variation sinusoidal. At inphase ($\phi = 2n\pi$, n = 1, 2, 3 …) flow where shear layers grow from the same side of the two cylinders, the growing shear layer of the downstream cylinder pulls the same-side growing shear layer of the upstream cylinder. Velocity in the same-side shear layer of the upstream cylinder thus increases. In the next half cycle of the vortex shedding period, velocity in the other-side shear layer is enhanced. C_{Lf} therefore becomes maximum at inphase flow. For antiphase ($\phi = (2n+1)\pi$) flow where shear layers grow from the opposite sides of the two cylinders, the growing shear layer of the downstream cylinder pulls the non-growing shear layer of the upstream cylinder, reducing the lift induced by the growing shear layer of the upstream cylinder. Minimum C_{Lf} thus prevails for antiphase flow. Pulling effect weakens at a larger L^*. The amplitude variation of C_{Lf} thus diminishes with L^*.

In the literature, it was known that ϕ is a linear function of L^*. The present investigation identifies that it is a function of L^*, St and $\overline{V_c}$, influencing the fluctuating component of the flow around and behind the upstream cylinder significantly. An equation of C_{Lf} is deduced as

$$C_{Lf} - C_{Lf0} = 13.8e^{-1.43L^*} + 0.36\,e^{-0.2L^*}\sin\left(\phi + \frac{\pi}{2}\right).$$

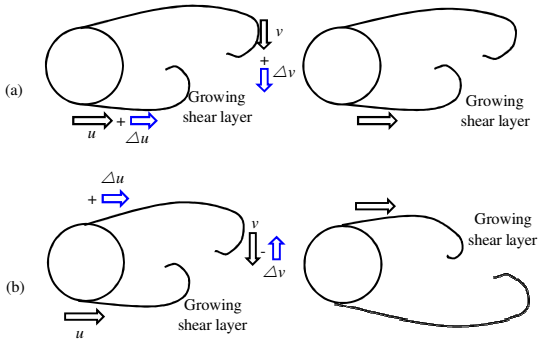

Figure. 7. A sketch showing the effect of shedding phase on the flow around the upstream cylinder. (a) Inphase flow, and (b) antiphase flow.

Acknowledgments

Alam wishes to acknowledge supports given to him from the Research Grant Council of Shenzhen Government through grants JCYJ20120613145300404 and JCYJ20130402100505796.

References

[1] Alam, M.M., Moriya, M., Takai, K. & Sakamoto, H., Fluctuating fluid forces acting on two circular cylinders in a tandem arrangement at a subcritical Reynolds number, *J. Wind Eng. Ind. Aerodyn*, **91**, 2003, 139-154.

[2] Alam, M.M., Sakamoto, H. & Zhou, Y., Effect of a T-shaped plate on reduction in fluid force on two tandem cylinders in a cross-flow, *J. Wind Eng. Ind. Aerodyn*, **94**, 2006, 525-551.

[3] Alam, M.M. & Zhou, Y., Phase lag between vortex shedding from two tandem bluff bodies, *J. Fluids Struct.*, **23**, 2007, 339-347.

[4] Dehkordi, B.G., Moghaddam, H.S., & Jafari, H.H., Numerical simulation of flow over two circular cylinders in tandem arrangement, *Comput. & Fluids.*, **23**, 2011, 114-126.

[5] Ding, H., Shu, C., Yeo, Y.O. & Xu, D., Numerical simulation of flows around twocircular cylinders by mesh-free least square-based finite difference methods, *Int. J. Numer. Meth. Fluids.*, **53**, 2007, 305–332.

[6] Koda, Y. & Lien, F., Aerodynamic effects of the early three-dimensional instabilities in the flow over one and two circular cylinders in tandem predicted by lattice Bolzmann method, *Computers & Fluids.*, **74**, 2013, 32-43.

[7] Sakamoto, H., Haniu, H. & Obata, Y., Fluctuating forces acting on two square prisms in a tandem arrangement., *J. Wind Eng. Ind. Aerodyn.*, **26**, 1987, 85–103.

[8] Zdravkovich, M.M., The effects of interference between circular cylinders in cross flow, *J. Fluid and Struct.*, **1**, 1987, 239-261.